ISSN: 2277-9655
Scientific Journal Impact Factor: 3.449
(ISRA), Impact Factor: 1.852

IJESRT

INTERNATIONAL JOURNAL OF ENGINEERING SCIENCES & RESEARCH TECHNOLOGY

Application of Trefftz method to Fluid Flow Problem

Ri-Song Qin[1], Yi Xiao[2*], Yong-Lan Yang[2]
[1]Fujian Port and Waterway Survey and Research Institute, 283 Yangqiao Road, Fuzhou, China
[2*]Research School of Engineering, Australian National University, Canberra, ACT 2601, Australia
[*]Corresponding author: yi.xiao@anu.edu.au

Abstract

The Trefftz method is widely used for solid mechanics applications since its mainstream introduction into the finite element approach approximately 40 years ago. The present investigation is to apply this technique to steady, imcompressible, non-turbulent, Newtonian fluid flow problems. We present a detailed process in developing F-Trefftz formulations for analyzing fluid flow problems. To verify the applicability and accuracy of the proposed models, three numerical examples are considered. The results obtained using both T-Trefftz and F-Trefftz methods are in high accuracy.
Keywords: Finite element method, Navier-Stokes flow, Trefftz method.

Introduction

In this paper the Trefftz method is used to solve the Navier-stokes problem. During the past decades, Trefftz numerical method, Trefftz finite element method in particular, has been considerably improved and has now become a highly efficient computational tool for the solutions of complex boundary-value problems [1-8]. Up to now, Trefftz-elements, or T-elements for short, have been successfully applied to problems of plane elasticity [9-11], Kirchhoff plates [1], moderately thick Reissner-Mindlin plates [3, 5], thick plates [4], geometrically nonlinear plates [12-14], as well as three-dimensional problems [15, 16], axisymmetric solid mechanics [12], open boundary problems [7], piezoelectric problems [17, 18], potential problems [19, 20], transient heat conduction and plate bending analysis [8, 21], minimal surface problems [22], biphasic elastostatics [23], problems with multiple vertical cylinders [24], elastic contact problems [25, 26], magnetic field analysis [27, 28], and materially nonlinear elasticity [29]. Further, the concept of special purpose functions has been found to be of great efficiency in dealing with various geometry or load-dependent singularities and local effects (e.g., obtuse or reentrant corners, cracks, circular or elliptic holes, concentrated or patch loads)[30-32]. A comprehensive discussion on this topic can be found in some review papers and books [33-35]. It should be mentioned that the finite element based on Trefftz functions can perform quite well for dealing with different types of problems to which it was applied. The main advantage of implementing the Trefftz method from a finite element standpoint is the possibility of combining the main features of the competing boundary element method [36, 37] and finite element methods [38-40]. The approximation bases are regular and the solving system is symmetric and sparse, like in the conforming finite element method but all structural matrices present boundary integral expressions, as in the conventional boundary element method [36].

Keeping the review and analysis above in mind, this paper describes the use of Trefftz functions to generate Trefftz numerical algorithms for Navier-stokes fluid equations. Several numerical examples are considered to show the applications of the proposed Trefftz formulation. The formulations and theories developed from this paper can serve as a theoretical basis for the development of Hybrid Trefftz finite element method and Trefftz boundary element methods for fluid-flow problems.

Basic equations and formulations

Governing equations and their boundary conditions

Navier-stokes equation is used as the governing equation for fluid flow problems in this paper. It is based on the principle of conservation of linear momentum for fluid. The motion of a non-turbulent, Newtonian incompressible fluid can be expressed as below:

$$-\nabla p + \mu \nabla^2 v + \rho b_k = \rho v \qquad (1)$$

where ρ denotes the density, v is the velocity vector,

ISSN: 2277-9655
Scientific Journal Impact Factor: 3.449
(ISRA), Impact Factor: 1.852

b_k is the body force.

In the absence of any body forces (b_k=0), the Stokes-flow equations governing the motion and continuity can be simplified as,

$$-\nabla p+\mu\nabla^2\mathbf{v}=0 \qquad (2)$$

$$\nabla\bullet\,\mathbf{v}=0 \qquad (3)$$

Eq (2) is the simplified governing equation and Eq (3) is the divergence of the velocity. In Eqs (2) and (3), $\mathbf{v}=v_1\mathbf{i}+v_2\mathbf{j}$ is the velocity vector, p is the pressure, and μ is the coefficient dynamic viscosity of the fluid. The Hamilton operator and Laplace operator for the case of two dimensional spaces are respectively [33]

$$\nabla=\frac{\partial}{\partial x}\mathbf{i}+\frac{\partial}{\partial y}\mathbf{j} \quad \text{(Hamilton operator)} \qquad (4)$$

$$\nabla^2=\nabla\bullet\nabla=\frac{\partial^2}{\partial x^2}+\frac{\partial^2}{\partial y^2} \quad \text{(Laplace operator)} \qquad (5)$$

In addition, to make the system complete, the following boundary conditions must be added

$$v_n=\bar{v}_n,\quad v_s=\bar{v}_s \qquad \text{on } S_v \qquad (6)$$

$$-p+2\mu\frac{\partial v_n}{\partial n}=\bar{p}_n,\quad \mu\left(\frac{\partial v_s}{\partial n}+\frac{\partial v_n}{\partial s}\right)=\bar{p}_s,\quad \text{on } S_p \qquad (7)$$

S_p is the surface on which forces are prescribed, and S_v is the surface on which velocity are prescribed. The velocity and surface boundary conditions are illustrated in Fig. 1.

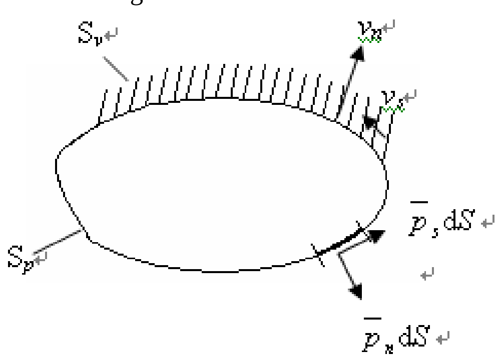

Fig. 1 Classification of boundary zones

Three essential formulations

In the literature there are three major formulations for solving multi-dimensional Navier–Stokes equations, or simply Stokes equations. They are: (1) primitive variables of velocity–pressure; (2) velocity–vorticity; and (3) vorticity–potential. In the following, we present the three essential formulations which can be taken as a basis in developing method of fundamental solution formulation.

Velocity-pressure formulation

Taking divergence of Eq (2) and making use of Eq (3), it is easy to see that the pressure p is harmonic, that is

$$\nabla\bullet\nabla p=\mu\nabla\bullet\nabla^2 v=\mu\nabla^2(\nabla\bullet v)=0\Leftrightarrow\nabla^2 p=0 \qquad (8)$$

Hence, through operating the Laplace operator on Eq (2), we find that the velocity vector $\mathbf{v}$ satisfies the equation

$$\begin{aligned}\mu\nabla^2\left(\nabla^2\mathbf{v}\right)&=\mu\nabla^4\mathbf{v}=\nabla^2\left(\nabla p\right)\\&=\nabla\left(\nabla^2 p\right)=0\Leftrightarrow\nabla^4\mathbf{v}=0\end{aligned} \qquad (9)$$

Velocity-vorticity formulation

By definition, the vorticity vector ω is expressed as

$$\boldsymbol{\omega}=\nabla\times\mathbf{v} \qquad (10)$$

Taking the curl to Eq (2) with constant μ, and using Eq (10), we obtain the steady-state vorticity transport equation for Stokes flows as follows [41]:

$$\begin{aligned}\nabla\times\left(-\nabla p+\mu\nabla^2\mathbf{v}\right)&=-\nabla\times\nabla p+\mu\nabla^2\left(\nabla\times\mathbf{v}\right)\\&=\mu\nabla^2\boldsymbol{\omega}=0\Leftrightarrow\nabla^2\boldsymbol{\omega}=0\end{aligned} \qquad (11)$$

Taking the curl to Eq (10) and using Eq (3) yields

$$\nabla\times\omega=\nabla\times(\nabla\times\mathbf{v})=\nabla(\nabla\cdot\mathbf{v})-\nabla^2\mathbf{v}=-\nabla^2\mathbf{v} \qquad (12)$$

Vorticity-potential formulation

The Helmholtz decomposition theorem [42] states that any vector can be written as the sum of two parts, one is curl-free and the other is solenoidal. In flow fields, the velocity is thereby decomposed into a potential flow and a viscous flow. In other words, the velocity $\mathbf{v}$ can be decomposed into the following form

$$\mathbf{v}=-\nabla\phi+\nabla\times\boldsymbol{\psi} \qquad (13)$$

where the scalar function ϕ is the velocity potential, and ψ represents the stream function vector and satisfies $\nabla\bullet\psi=0$ by its solenoidal definition.

Substituting the above equation into Eq (3) produces the Laplace equation for the velocity potential ϕ

$$\begin{aligned}\nabla\bullet v&=-\nabla\bullet(\nabla\phi)+\nabla\bullet(\nabla\times\psi)\\&=-\nabla^2\phi=0\Rightarrow\nabla^2\phi=0\end{aligned} \qquad (14)$$

Substituting Eq. (11) into Eq. (8) we can obtain

$$\omega=\nabla\times\mathbf{v}=\nabla\times(-\nabla\phi+\nabla\times\psi)=-\nabla^2\psi \qquad (15)$$

Further, applying the relation (11) for Eq (15) results in the final vector bi-harmonic equation for the stream function vector ψ

$$\nabla^4\psi=0 \qquad (16)$$

Application of method of fundamental solution to fluid flow

Method of fundamental solution (MFS)

MFS, also known as F-Trefftz method, has been studied for many years along with the boundary integral equation and boundary element method. The meshless MFS can get rid of the mesh generation and

ISSN: 2277-9655
Scientific Journal Impact Factor: 3.449
(ISRA), Impact Factor: 1.852

the numerical integration, thus MFS is much easier to implement than the indirect boundary element method, as far as numerical algorithm is concerned. MFS is based on the fundamental solutions of the governing equations, and its solution methodologies do not depend on the discretization of interior computational regions. The basic concept of the MFS is to decompose the solutions of the partial differential equations by superposition of the fundamental solutions with proper intensities. Wherein, the unknown coefficients can be obtained by the collocations of the boundary conditions. Since the MFS locates the source points outside the computational domain, no special treatments for the singularities of fundamental solutions are required. Therefore, the MFS is considered to be a grid-free scheme which depends only upon distances between pair of points of the so-called radial basis functions, thus MFS is more suitable for the exterior and irregular domain problems. MFS offers several advantages, first, meshing a boundary with only points is certainly much easier than with elements, second, singular integrals are avoided in the MFS (although singularities of the kernel still play a role), third, programming with the conventional MFS is significantly simplified compared with the boundary element method. All these advantages with the MFS have attracted continued interests from researchers [43-45].

Three types of MFS are described and compared here: the first one is the traditional MFS, using Stokeslets (Stokes operator) as the fundamental solution of the Stokes function, this work was done by Young et al. [46]; the second one is the MFS for stokes equations by the dual-potential formulation, it transforms the governing equation of the Stokes problem into velocity-verticity formulation form with free space Green's function as the fundamental solution, the third one also use the dual-potential formulation, but instead of using the Green's function, the field variable is approximated by a combination of a series of T-complete functions satisfying the governing equation. In this paper, we focus on the development of dual-potential method.

Dual-potential method

a) Dual-potential method with F-Trefftz Method

The dual-potential method is based on the combination of the Laplace equation for velocity potential and vector bi-harmonic equation for stream function vector by using the Helmholta decomposition theorem [46]. Here the velocity is written as two parts in the form given in Eq (13) by the Helmholtz decomposition theorem. As a result, ϕ and $\vec{\psi}$ can be obtained respectively using MFS from the Laplace equation, Eq (14), and vector bi-harmonic equation, Eq (16).

Here, the fundamental solution, also known as the free space Green's function is given by:

$$\zeta G(\vec{x};\vec{x}_0) = -\delta(\vec{x}-\vec{x}_0) \tag{17}$$

where ζ is a linear spatial differential operator, $\delta(\vec{x}-\vec{x}_0)$ is the well-known Dirac delta function, $\vec{x}=(x,y,z)$ is the position of the field point, $\vec{x}_0=(x_0,y_0,z_0)$ is the location of the source point, and the distance between a field point and a source point is defined by $r=|\vec{x}-\vec{x}_0|$. By applying Fourier transform theory to Eq (17), the fundamental solution of the 2D Laplace equation is obtained as [46]:

$$G_\phi(\vec{x};\vec{x}_0) = \frac{-1}{2\pi}\ln r \tag{18}$$

And the fundamental solution for 2D bi-harmonic equation can be written as:

$$G_\psi(\vec{x};\vec{x}_0) = \frac{-1}{8\pi} r^2 \ln r \tag{19}$$

The principle of superposition is employed for linear governing equations. Therefore in the spirit of MFS formulation the solution is represented by a series of fundamental solutions with singularities located outside the computational domain. The unknown coefficients of the series of fundamental solutions are regarded as the strengths of corresponding fundamental solutions [47]. Therefore the discretizations of stream function ψ and velocity potential ϕ are performed and represented as:

$$\psi(\vec{x}_i) = \sum_{j=1}^{N}\left[\alpha_j G_\psi(\vec{x}_i;\vec{x}_{0j})\right], \tag{20}$$

$$\phi(\vec{x}_i) = \sum_{j=1}^{N}\left[\beta_j G_\phi(\vec{x}_i;\vec{x}_{0j})\right], \tag{21}$$

where $\vec{x}_i$ is the i-th field point, $\vec{x}_{0j}$ is the j -th source point, N is the number of the source points and α_j and β_j, the unknown coefficients, are respectively associated with the fundamental solutions of stream function and velocity potential. Therefore, the velocity field is represented using Eq (13) as (here, $r_{ij}=|\vec{x}_i-\vec{x}_{0j}|$)[46]:

$$\begin{aligned} v_1(\vec{x}_i) = &\sum_{j=1}^{N}\left[\alpha_j(1+2\ln r_{ij})(y_i-y_{0j})\right] \\ &+\sum_{j=1}^{N}\left[\beta_j\frac{x_i-x_{0j}}{r_{ij}^2}\right] \end{aligned}, \tag{22}$$

ISSN: 2277-9655
Scientific Journal Impact Factor: 3.449
(ISRA), Impact Factor: 1.852

$$v_2(\vec{x}_i) = -\sum_{j=1}^{N}\left[\alpha_j(1+2\ln r_{ij})(x_i - x_{0j})\right] + \sum_{j=1}^{N}\left[\beta_j \frac{y_i - y_{0j}}{r_{ij}^2}\right] \tag{23}$$

The boundary conditions of velocity components are then collocated to find the unknown coefficients. It results in a $2N \times 2N$ linear system. After the $2N$ unknown coefficients of α_j and β_j are determined, we obtain the velocity first and then the vorticity fields. The vorticity field for 2D Stokes flow is shown as:

$$\zeta(\vec{x}_i) = -\sum_{j=1}^{N}\left[\alpha_j(4+4\ln r_{ij})\right] \tag{24}$$

b) Dual-potential method with T-complete function

In this work, we also use the so-called 'Dual-potential method', a general formulation by the dual-potential of velocity potential and stream function vector for Navier-Stokes equations is developed. Our attentions is mainly paid to the two-dimensional steady-state Stokes flow problems, and a boundary-type meshless collocation method is presented based on the Trefftz-complete, or T-complete for short, functions corresponding to Eqs (14) and (16). In the spirit of the Trefftz collocation method, the field variable is approximated by a combination of a series of T-complete functions satisfying the governing equation. So, the velocity potential ϕ and stream function ψ can be expressed as

$$\phi(\mathbf{x}) = \sum_{j=1}^{N}\alpha_j N_j^{\phi}(\mathbf{x}), \quad \psi(\mathbf{x}) = \sum_{j=1}^{N}\beta_j N_j^{\psi}(\mathbf{x}) \tag{25}$$

where $\mathbf{x} = (x_1, x_2)$ is the arbitrary point in the domain, N is the number of T-complete functions N_j^{ϕ} and N_j^{ψ}, which respectively satisfy 2D Laplace equation and bi-harmonic equation

$$\nabla^2 N_j^{\phi}(\mathbf{x}) = 0, \quad \nabla^4 N_j^{\psi}(\mathbf{x}) = 0 \tag{26}$$

and the unknown coefficients α_j and β_j are associated with T-complete functions of the velocity potential and stream function, respectively.

Next, the velocity field $\mathbf{v} = (v_1, v_2, 0)$ can be derived by way of Eq (13) as

$$v_1(\mathbf{x}) = -\frac{\partial\phi}{\partial x_1} + \frac{\partial\psi}{\partial x_2} = -\sum_{j=1}^{N}\alpha_j \frac{\partial N_j^{\phi}(\mathbf{x})}{\partial x_1} + \sum_{j=1}^{N}\beta_j \frac{\partial N_j^{\psi}(\mathbf{x})}{\partial x_2} \tag{27}$$

$$v_2(\mathbf{x}) = -\frac{\partial\phi}{\partial x_2} - \frac{\partial\psi}{\partial x_1} = -\sum_{j=1}^{N}\alpha_j \frac{\partial N_j^{\phi}(\mathbf{x})}{\partial x_2} - \sum_{j=1}^{N}\beta_j \frac{\partial N_j^{\psi}(\mathbf{x})}{\partial x_1} \tag{28}$$

Once the expressions of velocity components are given, the vorticity $\boldsymbol{\omega} = (0, 0, \omega)$ can be obtained by means of Eq (15), that is

$$\omega = -\nabla^2\psi = -\sum_{j=1}^{N}\beta_j \nabla^2 N_j^{\psi}(\mathbf{x}) \tag{29}$$

For the convenience of computation, we list the corresponding T-complete functions satisfying the Laplace equation and bi-harmonic equation, respectively, and its derivatives here[33, 48].

i) T-complete functions for Laplace equation in 2D bounded domain:

$$N_0^{\phi} = 1, \; N_1^{\phi} = r\cos\theta = x_1, \; N_2^{\phi} = r\sin\theta = x_2 \tag{30}$$

$$N_{2m-1}^{\phi} = r^m \cos(m\theta), \quad N_{2m}^{\phi} = r^m \sin(m\theta)$$

$$(m = 1, 2, \cdots) \tag{31}$$

Substituting these expressions into equation Eqs (27) and (28), we can obtain the first half of these formulations as follows:

$$\frac{\partial N_{2m-1}^{\phi}}{\partial x_1} = mr^{m-1}\cos(m-1)\theta,$$

$$\frac{\partial N_{2m-1}^{\phi}}{\partial x_2} = -mr^{m-1}\sin(m-1)\theta \tag{32}$$

$$\frac{\partial N_{2m}^{\phi}}{\partial x_1} = mr^{m-1}\sin(m-1)\theta,$$

$$\frac{\partial N_{2m}^{\phi}}{\partial x_2} = mr^{m-1}\cos(m-1)\theta \tag{33}$$

ii) T-complete functions for bi-harmonic equation in 2D bounded domain:

$$N_0^{\psi} = 1, \quad N_1^{\psi} = r^2, \; N_{4n-3}^{\psi} = \operatorname{Re} z^n, \quad N_{4n-2}^{\psi} = \operatorname{Im} z^n,$$

$$N_{4n-1}^{\psi} = r^2 \operatorname{Re} z^n, \; N_{4n}^{\psi} = r^2 \operatorname{Im} z^n \quad (n = 1, 2, \cdots)$$

$$r^2 = x_1^2 + x_2^2, \quad z = x_1 + ix_2$$

Substituting these expressions into Eqs (27) and (28), we can obtain the second half of these formulations as follows:

(1) $N_{4n-3}^{\psi} = \operatorname{Re} z^n$

$$\frac{\partial N_{4n-3}^{\psi}}{\partial x_1} = \operatorname{Re}\left(\frac{\partial z^n}{\partial x_1}\right) = \operatorname{Re}\left(\frac{\partial z^n}{\partial z}\frac{\partial z}{\partial x_1}\right) = \operatorname{Re}\left(nz^{n-1}\right) \tag{34}$$

$$\frac{\partial N_{4n-3}^{\psi}}{\partial x_2} = \operatorname{Re}\left(\frac{\partial z^n}{\partial x_2}\right) = \operatorname{Re}\left(\frac{\partial z^n}{\partial z}\frac{\partial z}{\partial x_2}\right) = \operatorname{Re}\left(niz^{n-1}\right) \tag{35}$$

(2) $N_{4n-2}^{\psi} = \operatorname{Im} z^n$

$$\frac{\partial N_{4n-2}^{\psi}}{\partial x_1} = \operatorname{Im}\left(\frac{\partial z^n}{\partial x_1}\right) = \operatorname{Im}\left(\frac{\partial z^n}{\partial z}\frac{\partial z}{\partial x_1}\right) = \operatorname{Im}\left(nz^{n-1}\right) \tag{36}$$

$$\frac{\partial N_{4n-2}^{\psi}}{\partial x_2} = \mathrm{Im}\left(\frac{\partial z^n}{\partial x_2}\right) = \mathrm{Im}\left(\frac{\partial z^n}{\partial z}\frac{\partial z}{\partial x_2}\right) = \mathrm{Im}\left(niz^{n-1}\right) \quad (37)$$

(3) $N_{4n-1}^{\psi} = r^2 \,\mathrm{Re}\, z^n = \mathrm{Re}\left(r^2 z^n\right)$

$$\frac{\partial N_{4n-1}^{\psi}}{\partial x_1} = \mathrm{Re}\left(\frac{\partial r^2 z^n}{\partial x_1}\right) = \mathrm{Re}\left(2x_1 z^n + r^2 \frac{\partial z^n}{\partial z}\frac{\partial z}{\partial x_1}\right) \quad (38)$$
$$= \mathrm{Re}\left(2x_1 z^n + r^2 n z^{n-1}\right)$$

$$\frac{\partial N_{4n-1}^{\psi}}{\partial x_2} = \mathrm{Re}\left(\frac{\partial r^2 z^n}{\partial x_2}\right) = \mathrm{Re}\left(2x_2 z^n + r^2 \frac{\partial z^n}{\partial z}\frac{\partial z}{\partial x_2}\right) \quad (39)$$
$$= \mathrm{Re}\left(2x_2 z^n + r^2 niz^{n-1}\right)$$

(4) $N_{4n}^{\psi} = r^2 \,\mathrm{Im}\, z^n = \mathrm{Im}\left(r^2 z^n\right)$

$$\frac{\partial N_{4n}^{\psi}}{\partial x_1} = \mathrm{Im}\left(\frac{\partial r^2 z^n}{\partial x_1}\right) = \mathrm{Im}\left(2x_1 z^n + r^2 \frac{\partial z^n}{\partial z}\frac{\partial z}{\partial x_1}\right) \quad (40)$$
$$= \mathrm{Im}\left(2x_1 z^n + r^2 n z^{n-1}\right)$$

$$\frac{\partial N_{4n}^{\psi}}{\partial x_2} = \mathrm{Im}\left(\frac{\partial r^2 z^n}{\partial x_2}\right) = \mathrm{Im}\left(2x_2 z^n + r^2 \frac{\partial z^n}{\partial z}\frac{\partial z}{\partial x_2}\right) \quad (41)$$
$$= \mathrm{Im}\left(2x_2 z^n + r^2 niz^{n-1}\right)$$

And the final system can be expressed as:

$$v_1(\mathbf{x}) = \left[-N_{1,1}^{\phi} \quad N_{1,2}^{\psi} \quad \cdots \quad \cdots \quad -N_{N,1}^{\phi} \quad N_{N,2}^{\psi}\right]\boldsymbol{\beta} \quad (42)$$
$$v_2(\mathbf{x}) = -\left[N_{1,2}^{\phi} \quad N_{1,1}^{\psi} \quad \cdots \quad \cdots \quad N_{N,2}^{\phi} \quad N_{N,1}^{\psi}\right]\boldsymbol{\beta} \quad (43)$$
$$\omega(\mathbf{x}) = \left[0 \quad -\nabla^2 N_1^{\psi} \quad \cdots \quad \cdots \quad 0 \quad -\nabla^2 N_N^{\psi}\right]\boldsymbol{\beta} \quad (44)$$

where $\boldsymbol{\beta} = \{\alpha_1, \beta_1, \ldots, \alpha_N, \beta_N\}^T$.

Enforcing Eqs (42)-(44) to satisfy the specified boundary conditions of velocity and vorticity can finally produce a system of linear equations, that is

$$\mathbf{H}\boldsymbol{\beta} = \mathbf{F} \quad (45)$$

from which all unknowns $\boldsymbol{\beta}$ can be determined. Once all coefficients are known, by means of Eqs (42)-(44) we can evaluate velocity components and vorticity at any point in the domain under consideration.

Here, comparing the related terms of T-complete functions of Laplace operator and Bi-harmonic operator, we can find that

$$-\frac{\mathrm{Im}\left(z^n\right)}{\partial x_1} = \frac{\mathrm{Re}\left(z^n\right)}{\partial x_2}, \qquad \frac{\mathrm{Re}\left(z^n\right)}{\partial x_1} = \frac{\mathrm{Im}\left(z^n\right)}{\partial x_2} \quad (46)$$

which means that there will be the same i^{th} and j^{th} columns in the final system matrix **H** due to the relationship that $-N_{i,1}^{\phi} = N_{j,2}^{\psi}$ and $-N_{i,2}^{\phi} = -N_{j,1}^{\psi}$, if all terms in T-complete functions of Laplace operator and Bi-harmonic operator are selected. As a result, the matrix is singular and can't be solved directly. To overcome this obstacle, we ignore the terms $N_{4n-2}^{\psi} = \mathrm{Re}\, z^n$ and $N_{4n-1}^{\psi} = \mathrm{Im}\, z^n$ in the set of T-complete functions of Bi-harmonic operator, and in order to keep the symmetry of terms, we also abandon the term r^2 in the practical computation. In a word, we employ the following terms to complete our computation

$$N_{2n-1}^{\phi} = \mathrm{Re}\left(z^n\right), \; N_{2n}^{\phi} = \mathrm{Im}\left(z^n\right) \quad (n = 1, 2, \cdots)$$
$$N_{2m-1}^{\psi} = r^2 \,\mathrm{Re}\, z^m, \; N_{2m}^{\psi} = r^2 \,\mathrm{Im}\, z^m \quad (m = 1, 2, \cdots)$$

Difference between the two dual-potential methods

There is major difference between the two dual-potential methods. First, as we mentioned above the function used in these two methods is different, F-Trefftz method use free space Green's function as the interpolation solution, and T-complete function method use T-complete function as the interpolation solution. Second, because we use collocation method here, the boundary conditions of the velocity components will be collocated for certain field points on the boundary in order to determine the unknown coefficients. In addition, these field points are selected in different way in these two methods. For F-Trefftz method, the fundamental solutions show singularity when the field point and source point overlap, so the usage of the fundamental solutions require special treatment of the location of source point, here, MFS avoid the singularity of the fundamental solutions by means of distributing source points outside the domain (Fig. 2). For T-complete function method, because T-complete functions are not singular at any time, the point can be choose along the boundary (Fig. 3).

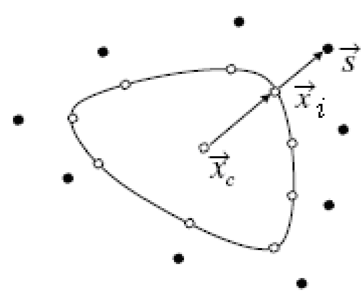

Fig. 2 Distribution of source and boundary field points in F-Trefftz method($\vec{s} = \vec{x}_i + b(\vec{x}_i - \vec{x}_c)$ ***)***

ISSN: 2277-9655
Scientific Journal Impact Factor: 3.449
(ISRA), Impact Factor: 1.852

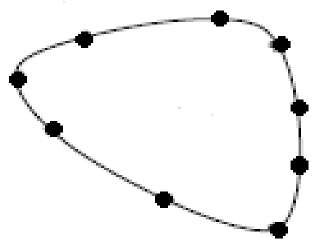

Fig. 3 Distribution field points in method of T-complete function

Numerical implementations

Unit square cavity (with F-Trefftz method)

Considering a unit square cavity filled with incompressible viscous Newton fluid, the solution of Stokes equations is given by

$$\mathbf{v}=\left(2xy,\ -y^2\right),\ \omega=-2x \text{ and } p=-2\mu y+p_0$$

which is also used to apply the velocity boundary conditions on the boundary. p_0 is a constant. The detailed description of the unit square cavity and related boundary conditions can be found in Fig. 4.

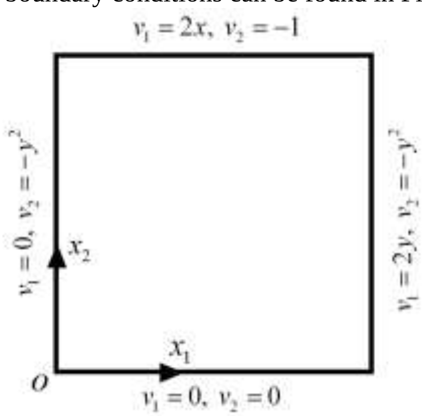

Fig. 4 Unit square cavity and related velocity boundary conditions

To solve this problem, first we need to determine the dimensionless parameter b and the number of points N used. For the value of *b*, we can find that in Fig. 5, the average absolute error (Aaerr) decreases when the value of *b* increases and the condition number (controlling the property of the solution of the function) increases when the value of *b* increases. It can be seen from Fig. 5 that larger value of *b* makes smaller Aaerr, but produces larger conditional number. Both of these two factors should be considered when we choose b. Based on the research reported in [49], we choose *b* = 0.5.

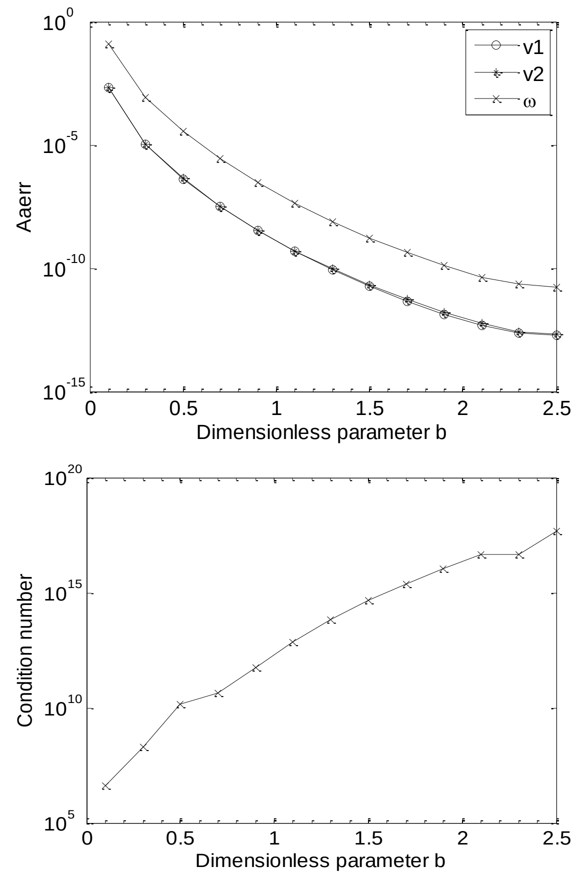

Fig. 5 Effect of dimensionless parameter b

How many collation points should be used is another key point, in addition to the selection of dimensionless parameter *b*. For the number of points *N* we also consider both the Aaerr and the conditional number, and here from Fig. 6 we can find that a suitable number for the collocation point is N=44.

After determining the value of *b* and *N*, we can obtain the actual solution of velocity and vorticity. Comparing with the analytical solution for these two vectors we can find that this method is very accurate in solving Navier-Stokes problems (Figs. 7 and 8).

ISSN: 2277-9655
Scientific Journal Impact Factor: 3.449
(ISRA), Impact Factor: 1.852

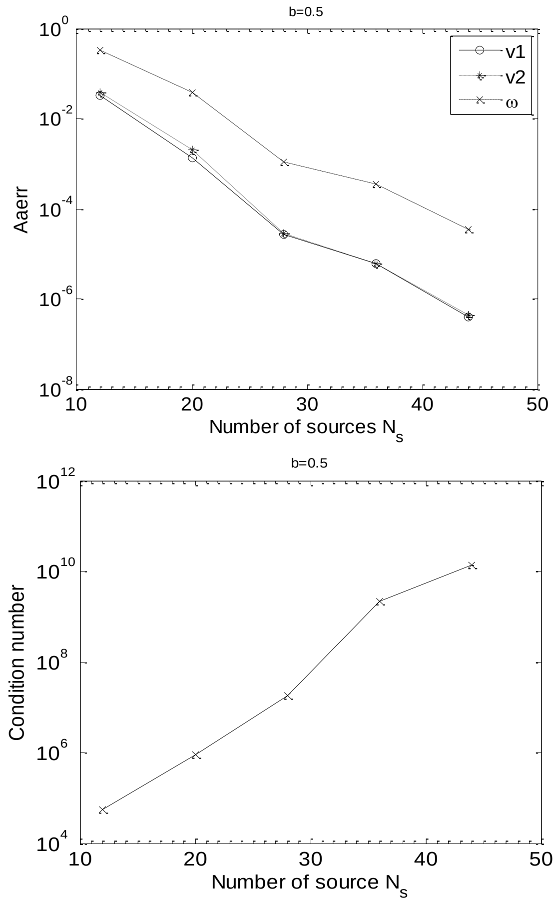

Fig. 6 Aaerr and condition number investigation with different number of source points

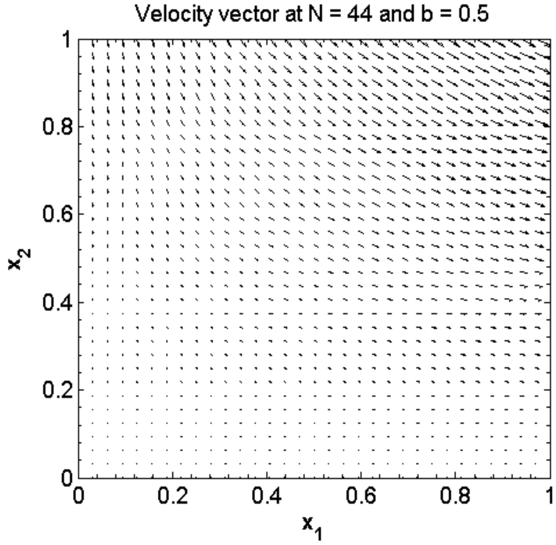

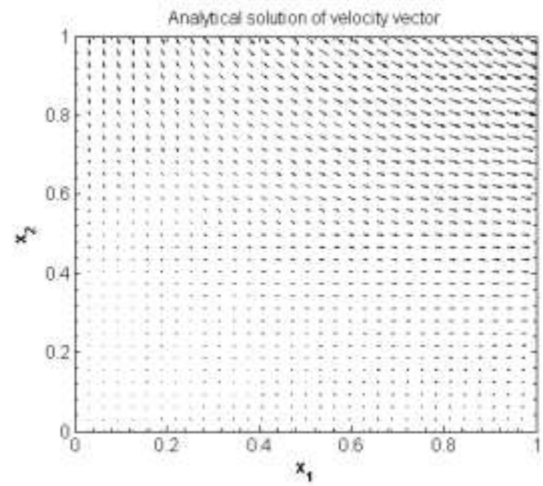

Fig. 7 Distribution of velocity

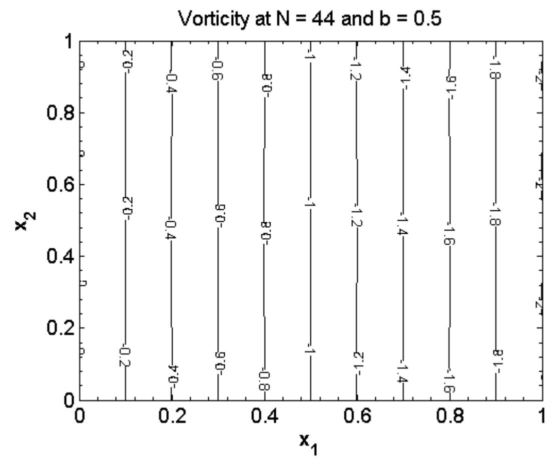

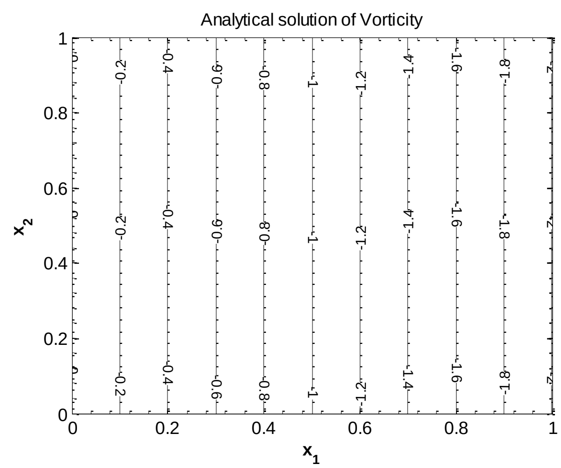

Fig. 8 Distribution of vorticity

Square cavity and Circular cavity

Having validated the accuracy of the proposed formulation, we apply it to two classic fluid problems to further assess the performance of the obtained

ISSN: 2277-9655
Scientific Journal Impact Factor: 3.449
(ISRA), Impact Factor: 1.852

models. First, considering a unit square cavity filled with incompressible viscous Newton fluid moving at a constant velocity on the top surface, and zero velocities applied on the other boundaries. The detailed description of the unit square cavity and related boundary conditions can be found in Fig. 9.

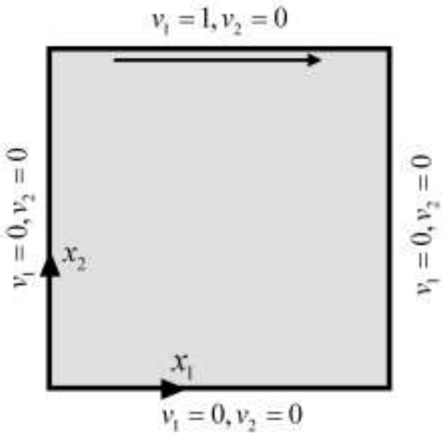

Fig. 9 Unit square cavity and related velocity boundary conditions

The process of choosing dimensionless parameter *b* and the number of collocation points is the same as we described above. For fluid problems, the distribution of velocity and vorticity within the domain are two main factors that we concerned, these two factors help us analysis the property of the fluid at each point inside the domain. After apply the method we can find the distribution of velocity and vorticity in the domain of the square cavity in Figs. 10 and 11.

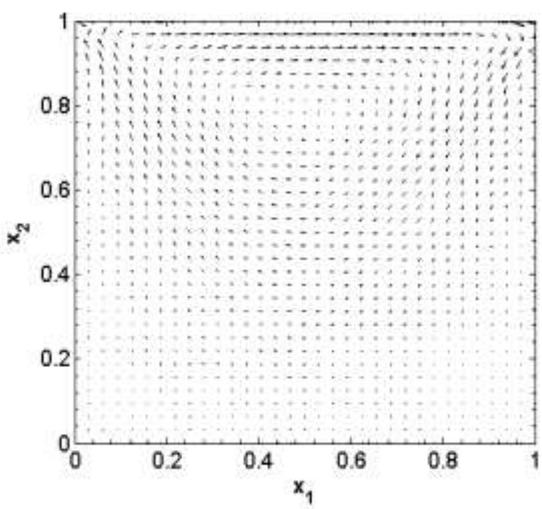

Fig. 10 Distribution of velocity vector in the square domain with N = 44 and b = 0.5

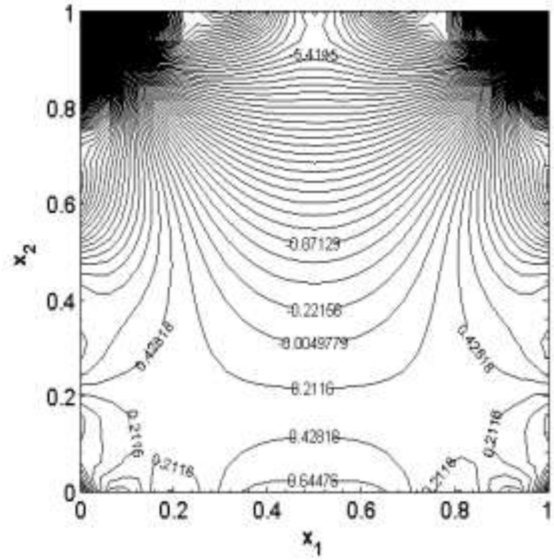

Fig. 11 Distribution of vorticity in the square domain with N = 44 and b = 0.5

The second numerical example is a recirculating flow in a 2D circular cavity. The radius of the circular cavity is assumed to be unity. The configuration and boundary conditions of the problem are shown in Fig. 12. In the upper half of the boundary, the velocity v_θ=1 in a anticlockwise sense and in the remainder, that is, lower half boundary, v_θ=0. In addition, the radial velocity v_r=0 is imposed on the entire boundary of the circular cavity.

$$v_x = v_r \cos\theta - v_\theta \sin\theta, v_y = v_r \sin\theta + v_\theta \cos\theta,$$

$$n = [\cos\theta, \sin\theta]$$

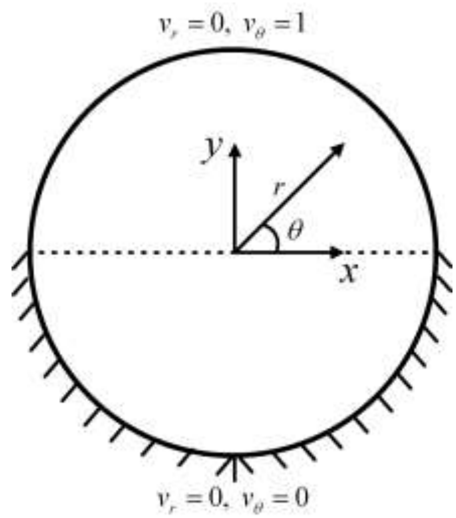

Fig. 12 Circular cavity and its boundary conditions

Fig. 13 shows the distribution of the source point and the field point, the point with a cross on it is source point and the one with a circle on it is a field point. Here we also focus on the velocity and vorticity of the problem, after the source point and the field point were selected, we collocated these points with F-Trefftz method and we can obtain the distribution of velocity and vorticity, shown in Figs. 14 and 15.

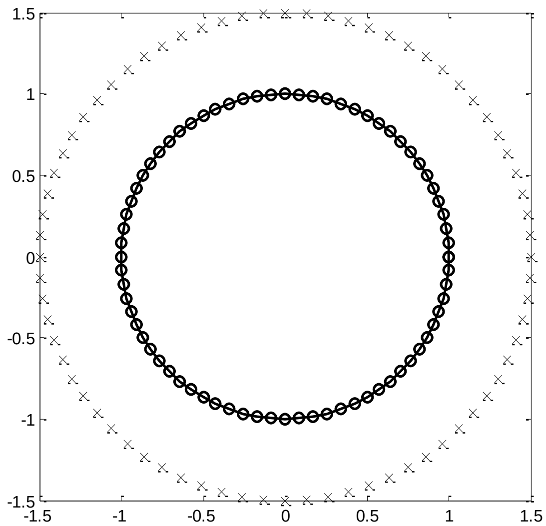

Fig. 13 Distribution of source point and field point

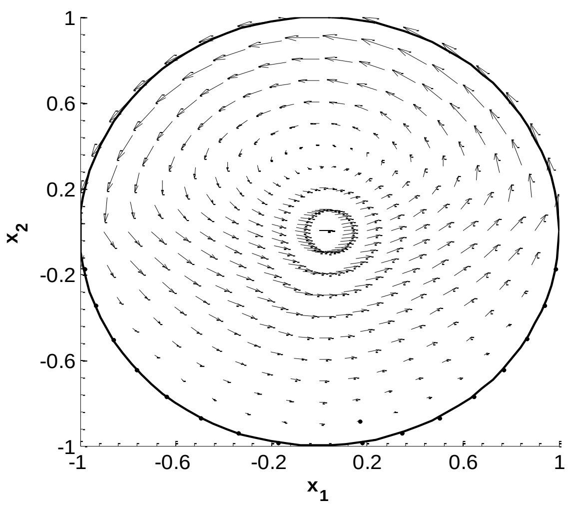

Fig. 14 Numerical distribution of velocity vector in a circular cavity

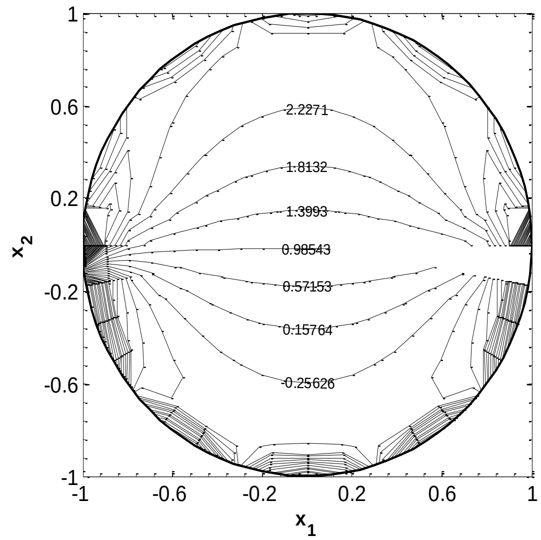

Fig. 15 Numerical distribution of verticity vector in a circular cavity

Conclusion

In this paper, the Trefftz method combined the use of the MFS interpolations was developed to solve the Navier-stokes fluid problems. Analysis on the fluid problem was performed and the numerical experiments were carried out to verify the efficiency and accuracy of this method. The key idea is to simplify the fundamental solutions of Stokes flows by the combination of the much simpler fundamental solutions of Laplace and bi-harmonic equations via the Helmholtz decomposition theorem. In this way, the unknown coefficients of both the velocity potential and the stream function vector are solved. Here, F-Trefftz method is applied to the following three examples, (1) a unite square cavity, (2) a square cavity and (3) a circular cavity. Comparing with solutions of analytical and numerical results, these numerical experiments demonstrate that the present scheme is accurate. In the future, weak form Trefftz method can be introduced into the solution of fluid flow problems with Trefftz finite element method (TFEM). Weak form TFEM is complicated than collocation method in the derivation of modified variational functional, and no work has been done in that area. Therefore, the solution derived from the TFEM method is expected to be more accurate, adaptive, and stable than the one we developed here.

References

[1] Qin QH. Hybrid Trefftz finite-element approach for plate bending on an elastic foundation. Applied Mathematical Modelling. 1994; 18:

334-339.
[2] Jirousek J, Ndiaye M. Solution of orthotropic plates based on para-extension of the hybrid-trefftz finite-element model. Computers & Structures. 1990; 34: 51-62.
[3] Jin F, Qin QH. A variational principle and hybrid Trefftz finite element for the analysis of Reissner plates. Computers & structures. 1995; 56: 697-701.
[4] Jirousek J, Wroblewski A, Qin QH, He X. A family of quadrilateral hybrid-Trefftz p-elements for thick plate analysis. Computer Methods in Applied Mechanics and Engineering. 1995; 127: 315-344.
[5] Qin QH. Hybrid-Trefftz finite element method for Reissner plates on an elastic foundation. Computer Methods in Applied Mechanics and Engineering. 1995; 122: 379-392.
[6] Qin QH. Postbuckling analysis of thin plates by a hybrid Trefftz finite element method. Computer Methods in Applied Mechanics and Engineering. 1995; 128: 123-136.
[7] Gyimesi M, Tsukerman I, Lavers D, Pawlak T, Ostergaard D. Hybrid finite element - Trefftz method for open boundary analysis. Ieee Transactions on Magnetics. 1996; 32: 671-674.
[8] Jirousek J, Qin QH. Application of hybrid-Trefftz element approach to transient heat conduction analysis. Computers & Structures. 1996; 58: 195-201.
[9] Qin QH. Dual variational formulation for Trefftz finite element method of elastic materials. Mechanics Research Communications. 2004; 31: 321-330.
[10] Lee CY, Qin QH, Wang H. Trefftz fnctions and application to 3D elasticity. Computer Assisted Mechanics and Engineering Sciences. 2008; 15: 251-263.
[11] Cao C, Qin QH, Yu A. Micromechanical Analysis of Heterogeneous Composites using Hybrid Trefftz FEM and Hybrid Fundamental Solution Based FEM. Journal of Mechanics. 2013; 29: 661-674.
[12] Qin QH. Nonlinear analysis of thick plates by HT FE approach. Computers & structures. 1996; 61: 271-281.
[13] Qin QH, Diao S. Nonlinear analysis of thick plates on an elastic foundation by HT FE with p-extension capabilities. International Journal of Solids and Structures. 1996; 33: 4583-4604.
[14] Qin QH. Postbuckling analysis of thin plates on an elastic foundation by HT FE approach. Applied Mathematical Modelling. 1997; 21: 547-556.
[15] Bussamra FLS, Lucena Neto E, Raimundo DS, Jr. Hybrid quasi-Trefftz 3-D finite elements for laminated composite plates. Computers & Structures. 2012; 92-93: 185-192.
[16] Dong L, Atluri SN. Development of 3D T-Trefftz Voronoi Cell Finite Elements with/without Spherical Voids &/or Elastic/Rigid Inclusions for Micromechanical Modeling of Heterogeneous Materials. CMC-Computers Materials & Continua. 2012; 29: 169-211.
[17] Qin QH. Variational formulations for TFEM of piezoelectricity. International Journal of Solids and Structures. 2003; 40: 6335-6346.
[18] Qin QH. Solving anti-plane problems of piezoelectric materials by the Trefftz finite element approach. Computational Mechanics. 2003; 31: 461-468.
[19] Sze KY, Liu GH. Hybrid-Trefftz six-node triangular finite element models for Helmholtz problem. Computational Mechanics. 2010; 46: 455-470.
[20] Wang H, Qin QH, Liang XP. Solving the nonlinear Poisson-type problems with F-Trefftz hybrid finite element model. Engineering Analysis with Boundary Elements. 2012; 36: 39-46.
[21] Qin QH. Transient plate bending analysis by hybrid Trefftz element approach. Communications in Numerical Methods in Engineering. 1996; 12: 609-616.
[22] Wang H, Qin QH, Arounsavat D. Application of hybrid Trefftz finite element method to non‐linear problems of minimal surface. International journal for numerical methods in engineering. 2007; 69: 1262-1277.
[23] Moldovan ID, Cao TD, Teixeira de Freitas JA. Hybrid-Trefftz finite elements for biphasic elastostatics. Finite Elements in Analysis and Design. 2013; 66: 68-82.
[24] Stojek M, Markiewicz M, Mahrenholtz O. Diffraction loads on multiple vertical cylinders with rectangular cross section by Trefftz-type finite elements. Computers & Structures. 2000; 75: 335-345.
[25] Wang K, Qin QH, Kang Y, Wang J, Qu C. A direct constraint‐Trefftz FEM for analysing elastic contact problems. International journal for numerical methods in engineering. 2005; 63: 1694-1718.
[26] Qin QH, Wang KY. Application of hybrid-Trefftz finite element method to frictional contact problems. Computer Assisted Mechanics and Engineering Sciences. 2008; 15: 319-336.
[27] Onuki T, Wakao S, Kuwahara T, Im JW. Hybrid

ISSN: 2277-9655
Scientific Journal Impact Factor: 3.449
(ISRA), Impact Factor: 1.852

Trefftz and finite element method applied to magnetic field analysis for rotating machines. Ieee Transactions on Magnetics. 1997; 33: 2014-2017.

[28] Olegovich Y. Trefftz finite elements for electromagnetics. IEEE Transactions on Microwave Theory and Techniques. 2002; 50: 1328-1339.

[29] Qin QH. Formulation of hybrid Trefftz finite element method for elastoplasticity. Applied mathematical modelling. 2005; 29: 235-252.

[30] Dhanasekar M, Han J, Qin QH. A hybrid-Trefftz element containing an elliptic hole. Finite Elements in Analysis and Design. 2006; 42: 1314-1323.

[31] Qin QH, He XQ. Special elliptic hole elements of Trefftz FEM in stress concentration analysis. Journal of Mechanics and MEMS. 2009; 1: 335-348.

[32] Wang H, Qin QH. A new special element for stress concentration analysis of a plate with elliptical holes. Acta Mechanica. 2012; 223: 1323-1340.

[33] Qin QH. The Trefftz Finite and Boundary Element Method. Southampton: WIT Press; 2000.

[34] Qin QH. Trefftz finite element method and its applications. Applied Mechanics Reviews. 2005; 58: 316-337.

[35] Qin QH, Wang H. Matlab and C programming for Trefftz finite element methods: CRC Press, Taylor & Francis, Boca Raton; 2008.

[36] Qin QH. Nonlinear analysis of Reissner plates on an elastic foundation by the BEM. International Journal of Solids and Structures. 1993; 30: 3101-3111.

[37] Qin QH, Mai YW. BEM for crack-hole problems in thermopiezoelectric materials. Engineering Fracture Mechanics. 2002; 69: 577-588.

[38] Bathe KJ. Finite element procedures. New Jersey: Prentice-Hall, Inc. ; 1996.

[39] Qin QH, Mao CX. Coupled torsional-flexural vibration of shaft systems in mechanical engineering—I. Finite element model. Computers & Structures. 1996; 58: 835-843.

[40] Qin QH, He XQ. Variational principles, FE and MPT for analysis of non-linear impact-contact problems. Computer methods in applied mechanics and engineering. 1995; 122: 205-222.

[41] Leita VMA. Applications of multi-region Trefftz-collocation to fracture mechanics. Engineering Analysis with Boundary Elements. 1998; 22: 251-256.

[42] Li ZC, Lu TT, Hu HY. The collocation Trefftz method for biharmonic equations with crack singularities. Engineering Analysis with Boundary Elements. 2004; 28: 79-96.

[43] Wang H, Qin QH. Meshless approach for thermo-mechanical analysis of functionally graded materials. Engineering Analysis with Boundary Elements. 2008; 32: 704-712.

[44] Wang H, Qin QH, Some problems with the method of fundamental solution using radial basis functions. Acta Mechanica Solida Sinica. 2007; 20: 21-29.

[45] Zhang ZW, Wang H, Qin QH, Method of fundamental solutions for nonlinear skin bioheat model. Journal of Mechanics in Medicine and Biology. 2014; 14 (4): 1450060.

[46] Young DL, Chiua CL. Method of fundamental solutions for multidimensional Stokes equations by the dual-potential formulation. European Journal of Mechanics B/Fluids. 2006; 25: 877–893.

[47] de Freitas JAT, LeitaÄo VMA. A boundary integral Trefftz formulation with symmetric collocation. Computational Mechanics. 2000; 25: 515-523.

[48] Zienkiewicz OC. Trefftz type approximation and the generalized finite element method-history and development. Computer Assisted Mechanics and Engineering Sciences. 1997; 4: 305-316.

[49] Jirousek J, Venkatesh A. A new FE approach for adaptive reliability assurance. Computers & Structures. 1990; 37: 217-230.